Adiabatic formulation of models

By **Terry Davies**

Table of contents

1. Introduction

These notes are not a verbatim record of the lecture series, but rather a condensation of the topics covered. They describe some of the techniques used in the adiabatic formulation of primitive-equation models of the atmosphere. Some sections have been taken directly from earlier notes by D. Burridge and from a paper by A. Simmons and D. Dent. These notes are not complete and need to be supplemented by the following sources:

(i) 'Numerical prediction and dynamic meteorology' by Haltiner and Williams. This is a very useful textbook and reference book describing many of the basic principles and techniques used in NWP.

(ii) 'Numerical methods for weather prediction', ECMWF Seminar notes 1983 and, in particular, chapters by Mesinger, Janjic and Arakawa. Unfortunately this volume is out of print but you may be able to find a copy in your home institution.

In addition to the above, useful material can also be found in Philips's article in 'Planetary fluid dynamics' edited by P. Morel and 'Numerical methods used in atmospheric models' by Mesinger and Arakawa, Garp Publications Series No. 17, Volume 1, (1976).

2. Governing equations

Taking an inertial (or fixed) frame of reference, Newton's second law can be expressed as

$$\frac{\mathrm{D}\mathbf{V}_\mathrm{a}}{\mathrm{D}t} = \mathbf{F} \tag{1}$$

where $\mathbf{F}$ is the sum of all the forces per unit mass. $\mathbf{V}_\mathrm{a}$ is the velocity as observed in the inertial frame. We need to express this equation in a reference frame on earth and which rotates with the earth.

Let Ω be the angular velocity of the earth, then

$$\mathbf{V}_\mathrm{a} = \mathbf{V} + \Omega \times \mathbf{r} \tag{2}$$

where $\mathbf{V}$ is the velocity relative to the earth and $\mathbf{r}$ represents the position vector of the particle as measure from the origin at the earth's centre.

Now consider the time derivative of a vector $\mathbf{V} = \mathbf{V}'_x\mathbf{i}' + \mathbf{V}'_y\mathbf{j}' + \mathbf{V}'_z\mathbf{k}'$ in the inertial frame and $\mathbf{V} = \mathbf{V}_x\mathbf{i} + \mathbf{V}_y\mathbf{j} + \mathbf{V}_z\mathbf{k}$ in the rotating frame where $\mathbf{i}'$, $\mathbf{j}'$, $\mathbf{k}'$ and $\mathbf{i}$, $\mathbf{j}$, $\mathbf{k}$ are unit vectors along the orthogonal axes in the two frames. Thus

$$\begin{aligned}\frac{\mathrm{D}\mathbf{V}}{\mathrm{D}t} &= \frac{\mathrm{d}\mathbf{V}'_x}{\mathrm{d}t}\mathbf{i}' + \frac{\mathrm{d}\mathbf{V}'_y}{\mathrm{d}t}\mathbf{j}' + \frac{\mathrm{d}\mathbf{V}'_z}{\mathrm{d}t}\mathbf{k}' \\ &= \frac{\mathrm{d}\mathbf{V}_x}{\mathrm{d}t}\mathbf{i} + \frac{\mathrm{d}\mathbf{V}_y}{\mathrm{d}t}\mathbf{j} + \frac{\mathrm{d}\mathbf{V}_z}{\mathrm{d}t}\mathbf{k} + \mathbf{V}_x\frac{\mathrm{d}\mathbf{i}}{\mathrm{d}t} + \mathbf{V}_y\frac{\mathrm{d}\mathbf{j}}{\mathrm{d}t} + \mathbf{V}_z\frac{\mathrm{d}\mathbf{k}}{\mathrm{d}t}\end{aligned}$$

Now $\mathrm{d}\mathbf{i}/\mathrm{d}t = \Omega \times \mathbf{i}$, etc. so that we can write

$$\frac{\mathrm{D}\mathbf{V}}{\mathrm{D}t} = \frac{\mathrm{d}\mathbf{V}}{\mathrm{d}t} + \Omega \times \mathbf{V} \tag{3}$$

Using the expression in (1) and using (2) we can show that

$$\frac{\mathrm{D}\mathbf{V}_\mathrm{a}}{\mathrm{D}t} = \frac{\mathrm{d}\mathbf{V}}{\mathrm{d}t} + 2\Omega \times \mathbf{V} + \Omega \times (\Omega \times \mathbf{r})$$

The second term of the right-hand side is the Coriolis force and the third term the centrifugal force. In atmospheric motions, the forces we are concerned with are those of gravitation, friction and pressure. Normally, the centrifugal force is included in the gravitational force which is taken as constant $= g\mathbf{k}$.

The equation of motion can be written as

$$\frac{\mathrm{d}V}{\mathrm{d}t} = -\alpha\nabla p - 2\Omega \times \mathbf{V} - g\mathbf{k} + \mathbf{F} \tag{4}$$

where **F** denotes the frictional force and $\alpha = 1/\rho$ is the specific volume, ρ is the density. The equation of mass continuity expresses the fact that local density changes are brought about by mass divergence.

$$\frac{\partial\rho}{\partial t} = -\nabla\cdot\rho\mathbf{V} \tag{5}$$

or, alternatively, $\mathrm{d}\rho/\mathrm{d}t = -\rho\nabla\cdot\mathbf{V}$.

The first law of thermodynamics can be written

$$Q = \frac{\mathrm{d}I}{\mathrm{d}t} + p\frac{\mathrm{d}\alpha}{\mathrm{d}t} \tag{6}$$

where Q is the heating or cooling from diabatic effects, $\mathrm{d}I/\mathrm{d}t$ is the rate of change of internal energy and $p(\mathrm{d}\alpha/\mathrm{d}t)$ represents the work done by expansion.

For a perfect gas, $I = C_{\mathrm{v}}T$ and we have the equation state of

$$p = R\rho T \tag{7}$$

where $R = C_p - C_{\mathrm{v}}$ is the gas constant and C_p and C_{v} are the specific heats at constant pressure and volume, respectively.

Using $I = C_{\mathrm{v}}T$ we can rewrite (6) as

$$Q = C_{\mathrm{v}}\frac{\mathrm{d}T}{\mathrm{d}t} + p\frac{\mathrm{d}\alpha}{\mathrm{d}t} \tag{8}$$

Alternatively, we can expand $p\frac{\mathrm{d}\alpha}{\mathrm{d}t} = p\frac{\mathrm{d}}{\mathrm{d}t}\left(\frac{RT}{p}\right) = R\frac{\mathrm{d}T}{\mathrm{d}t} - \frac{RT}{p}\frac{\mathrm{d}p}{\mathrm{d}t}$ and rearranging (8) we have

$$Q = C_p\frac{\mathrm{d}T}{\mathrm{d}t} - \frac{RT}{p}\omega \ , \tag{9}$$

where $\omega = \mathrm{d}p/\mathrm{d}t$.

In terms of potential temperature $\Theta = (p_0/p)^{\kappa}T$ (or $T = \Pi\Theta$ where $\Pi = (p/p_0)^{\kappa}$) where $\kappa = R/C_p$, $p_0 = 1000$ hPa.

We have $C_p\frac{\mathrm{d}\Theta}{\mathrm{d}t} = C_p\Pi\frac{\mathrm{d}\Theta}{\mathrm{d}t} + C_p\Theta\frac{\kappa}{p}\Pi\frac{\mathrm{d}p}{\mathrm{d}t}$ and, on substituting in (9), and rearranging we find

$$C_p\frac{\mathrm{d}\Theta}{\mathrm{d}t} = \frac{\Theta}{T}Q \tag{10}$$

2.1 Horizontal coordinate systems

Application of the equations of motion requires the use of an appropriate coordinate system. The obvious choice for global models is to choose spherical polar coordinates with longitude λ, latitude φ and radial distance r. The map factors in this system are $h_{\lambda} = r\cos\varphi$, $h_{\varphi} = r$, $h_r = 1$ and the velocity components are

$$u = h_\lambda \frac{d\lambda}{dt} = r\cos\varphi \frac{d\lambda}{dt} \text{ , the eastward component}$$

$$v = h_\varphi \frac{d\varphi}{dt} = r\frac{d\varphi}{dt} \text{ , the northward component}$$

$$w = h_r \frac{dr}{dt} = \frac{dr}{dt} \text{ , the radial component,}$$

The radial distance $r = a + z$ where a is the radius of the earth and z is the vertical distance above the surface of the earth.

The components of the momentum equation become

$$\frac{du}{dt} = 2\Omega v \sin\theta - 2\Omega w \cos\varphi + \frac{uv\tan\varphi}{r} - \frac{uw}{r} - \frac{1}{\rho r\cos\varphi}\frac{\partial p}{\partial\lambda} + F_\lambda \quad (11)$$

$$\frac{dv}{dt} = -2\Omega u \sin\varphi - \frac{u^2\tan\varphi}{r} - \frac{vw}{r} - \frac{1}{\rho r}\frac{\partial p}{\partial\varphi} + F_\varphi \quad (12)$$

$$\frac{dw}{dt} = 2\Omega u \cos\varphi + \frac{u^2 + v^2}{r} - \frac{1}{\rho}\frac{\partial p}{\partial r} - g + F_z \quad (13)$$

where

$$\frac{d}{dt} = \frac{\partial}{\partial t} + \frac{u}{a\cos\varphi}\frac{\partial}{\partial\lambda} + \frac{v}{a}\frac{\partial}{\partial\varphi} + w\frac{\partial}{\partial r}$$

From equations (11), (12) and (13), it can be shown that

$$\frac{d}{dt}\left(\frac{1}{2}\mathbf{V}^2\right) = \mathbf{V}\cdot\left(-\frac{1}{\rho}\nabla p + \mathbf{F} - g\mathbf{k}\right) \quad (14)$$

i.e. the rate of change of kinetic energy is equal to the rate at which the forces of pressure friction and gravity do work.

We can also show that

$$\frac{d}{dt}[(u + \Omega r\cos\varphi)r\cos\varphi] = r\cos\varphi\left(-\frac{1}{\rho r\cos\varphi}\frac{\partial p}{\partial\lambda} + F_\lambda\right) \quad (15)$$

which is the angular momentum principle.

For long integrations e.g. climate runs, it is important that these principles are maintained.

In the study of larger-scale atmospheric motions, at least for motions we are usually concerned with in numerical modelling, the following approximations can be justified.

(i) Since $z \ll a$, we replace r by the constant value a.

(ii) The Coriolis and metric terms proportional to $\cos\varphi$ are ignored.

(iii) We make the hydrostatic approximation to equation (13) so that

$$\frac{\partial p}{\partial z} = -\rho g \qquad (16)$$

i.e. the gravity force balances the vertical pressure gradient force.

Under these assumptions,

$$u = a\cos\varphi\frac{\mathrm{d}\lambda}{\mathrm{d}t}, \quad v = a\frac{\mathrm{d}\varphi}{\mathrm{d}t}, \quad w = \frac{\mathrm{d}z}{\mathrm{d}t} \qquad (17)$$

$$\frac{\mathrm{d}u}{\mathrm{d}t} = -\frac{1}{\rho a\cos\varphi}\frac{\partial p}{\partial\lambda} + fv + uv\frac{\tan\varphi}{a} + F_\lambda \qquad (18)$$

$$\frac{dv}{dt} - \frac{1}{\rho a}\frac{\partial p}{\partial\varphi} - fu - u^2\frac{\tan\varphi}{a} + F_\varphi \qquad (19)$$

$$\frac{\partial p}{\partial z} = -\rho g \qquad (20)$$

where $f = 2\Omega\sin\varphi$ is the Coriolis parameter.

Equations (18), (19), (20) together with the continuity equation (5), the equation of state (7) and the thermodynamic equation ((8), (9) or (10)) give us the required number of equations for the unknowns u, v, w, p, ρ, T ; these are known collectively as the primitive equations.

However, there is no prediction equation for w since we ignore vertical accelerations ($\mathrm{d}w/\mathrm{d}t$) by our use of the hydrostatic approximation. w is usually diagnosed from a form of the continuity equation.

2.2 The shallow water equations

The primitive equations are nonlinear, and it is only possible to solve them approximately using numerical methods. Some of the properties of the primitive equations, and also of the numerical schemes used in their solution, can be examined by studying simplified forms of the equations.

One such set of equations are the shallow water equations.

If we assume constant density, the horizontal pressure force in the equations of motion is independent of height so that

$$\nabla p = \rho g\nabla h \qquad (21)$$

where h is the height of the free surface.

If we further assume that the velocity field is initially independent of height, then it will remain so and consequently we can omit the vertical advection terns.

We also assume that the fluid is incompressible so that the continuity equation is

$$\nabla\cdot\mathbf{V} + \frac{\partial w}{\partial z} = 0 \qquad (22)$$

which can be integrated from $z = 0$ to $z = h$ (the bottom to the free top surface) to give

$$h\nabla\cdot\mathbf{V}+w_h-w_0 = 0 \quad (23)$$

At the bottom $w_0 = 0$ whilst at the top, $w_h = \mathrm{d}h/\mathrm{d}t$, the rate at which the free surface rises or falls.

Thus

$$w_h = \frac{\partial h}{\partial t}+\mathbf{V}\cdot\nabla h = -h\nabla\cdot\mathbf{V} \quad (24)$$

or

$$\frac{\partial h}{\partial t}+\mathbf{V}\cdot\nabla h+h\nabla\cdot\mathbf{V} = 0$$

The set of equations is completed by the momentum equations which are

$$\frac{\partial\mathbf{V}}{\partial t}+\mathbf{V}\cdot\nabla\mathbf{V}+f\mathbf{k}\times\mathbf{V}+g\nabla h = 0 \quad (25)$$

The equations of motion above are in a form known as the advective form due to the presence of the $\mathbf{V}\cdot\nabla\mathbf{V}$ term. The equations of motion can easily be rearranged into their vector invariant form viz:

$$\frac{\partial\mathbf{V}}{\partial t}+(\zeta+\boldsymbol{f})\mathbf{k}\times\mathbf{V}+\nabla(gh+E) = 0 \quad (26)$$

where

$$\zeta = \frac{1}{a\cos\varphi}\left(\frac{\partial v}{\partial\lambda}-\frac{\partial}{\partial\varphi}(u\cos\varphi)\right)$$

is the vorticity in spherical coordinates (cf. with $\zeta = \partial v/\partial x-\partial u/\partial y$ in a Cartesian system) and $E = 0.5(u^2+v^2)$ is the kinetic energy.

The equations of motion can be combined and rearranged into their vorticity/divergence form. Consider the shallow water equations in a Cartesian system where the vorticity is $\zeta = \partial v/\partial x-\partial u/\partial y$.

$$\begin{aligned}\frac{\partial u}{\partial t}+u\frac{\partial u}{\partial x}+v\frac{\partial u}{\partial y}-fv+g\frac{\partial h}{\partial x} &= 0\\ \frac{\partial v}{\partial t}+u\frac{\partial v}{\partial x}+v\frac{\partial v}{\partial y}+fu+g\frac{\partial h}{\partial y} &= 0\end{aligned} \quad (27)$$

Operating on the v-equation by $\partial/\partial x$, the u-equation by $\partial/\partial y$ and subtracting, we obtain

$$\frac{\partial\zeta}{\partial t}+\nabla\cdot[(\zeta+f)\mathbf{V}] = 0 \quad (28)$$

The divergence can be obtained by operating on the u-equation by $\partial/\partial x$ and the v-equation by $\partial/\partial y$ and adding to obtain

$$\frac{\partial D}{\partial t} + \nabla \cdot [(\zeta + f)k \times V] + \nabla^2\left(gh + \frac{u^2 + v^2}{2}\right) = 0 \qquad (29)$$

2.3 Map projections

So far, we have used a spherical polar coordinate system in our derivation of the primitive equations. However, it is sometimes necessary to map onto a plane. This is often done for limited-area modelling and, of course, is necessary when producing charts.

The advective form of the shallow water equations in a generalized linear coordinate system x, y with corresponding map factors h_x and h_y are

$$\frac{\partial u}{\partial t} + \frac{u}{h_x}\frac{\partial u}{\partial x} + \frac{v}{h_y}\frac{\partial u}{\partial y} - v\left[f + \frac{1}{h_x h_y}\left(v\frac{\partial h_y}{\partial x} - u\frac{\partial h_x}{\partial y}\right)\right] + \frac{g}{h_x}\frac{\partial h}{\partial x} = 0 \qquad (30)$$

$$\frac{\partial v}{\partial t} + \frac{u}{h_x}\frac{\partial v}{\partial x} + \frac{v}{h_y}\frac{\partial v}{\partial y} + u\left[f + \frac{1}{h_x h_y}\left(v\frac{\partial h_y}{\partial x} - u\frac{\partial h_x}{\partial y}\right)\right] + \frac{g}{h_x}\frac{\partial h}{\partial y} = 0 \qquad (31)$$

$$\frac{\partial h}{\partial t} + \frac{1}{h_x h_y}\left[\frac{\partial}{\partial x}(h_y u h) + \frac{\partial}{\partial y}(h_x v h)\right] = 0 \qquad (32)$$

In this system, the vorticity ζ and divergence D are given by

$$\zeta = \frac{1}{h_x h_y}\left[\frac{\partial}{\partial x}(h_y v) - \frac{\partial}{\partial y}(h_x u)\right] \qquad (33)$$

$$D = \frac{1}{h_x h_y}\left[\frac{\partial}{\partial x}(h_y u) + \frac{\partial}{\partial y}(h_x v)\right] \qquad (34)$$

When $h_x = h_y$, the angles between intersecting curves are preserved and the system is conformal.

We have already shown that a spherical polar coordinate system has $h_\lambda = a\cos\varphi$, $h_\varphi = a$.

2.3 (a) Polar stereographic projection. This projection is used for maps and was widely used in modelling in limited area models and the hemispheric domain. If r is the radius of a latitude circle on the map then

$$r = 2a\tan\frac{\Phi}{2}, \qquad \text{where } \Phi = \frac{\pi}{2} - \varphi \qquad (35)$$

The longitudinal angle is defined as $\Theta = \lambda$ so that with (x, y) axes with origin at the pole, x positive eastwards, y positive northwards from our reference longitude, then $x = r\sin\Theta$ and $y = r\cos\Theta$. In terms of φ and λ these become

$$x = \frac{2a\cos\varphi\sin\lambda}{(1 + \sin\varphi)}, \qquad y = -\frac{2a\cos\varphi\cos\lambda}{(1 + \sin\varphi)} \qquad (36)$$

with $r = am(\varphi)\cos\varphi$, where $m(\varphi) = 2/(1 + \sin\varphi)$ is the map factor ($h_x = h_y = 1/m(\varphi)$). The wind components (u, v) in the (x, y) directions are $u = h_x\dot{x}, v = h_y\dot{y}$ and are related to the velocities (u_s, v_s) in the spherical system by $u = u_s\cos\lambda - v_s\sin\lambda$ and $v = u_s\sin\lambda + v_s\cos\lambda$.

2.3 (b) Mercator (cylindrical) projection. This is commonly used for maps or for modelling in tropical regions. The x (east–west) and y (north–south) coordinates are defined by

$$x = a\cos\varphi_0\lambda, \qquad y = a\cos\varphi_0 \ln\left(\frac{1+\sin\varphi}{\cos\varphi}\right) \tag{37}$$

where φ_0 is the latitude at which the projection is true (usually $\varphi_0 = 0$, the equator). The map factor $m(\varphi) = \dfrac{\cos\varphi_0}{\cos\varphi} = \dfrac{1}{h_x} = \dfrac{1}{h_y}$.

3. Horizontal discretization

So far, we have derived the basic hydrodynamical equations that govern atmospheric motions. Given the initial fields of mass and velocity it is possible to treat the solution of these equations as an initial value problem and thus obtain the mass and velocity distribution at some future time. However, the partial differential equations are nonlinear and can only be solved by using numerical techniques. Furthermore, the nonlinearity of the equations means that any small errors in the initial conditions are likely to grow, making the solution useless in a deterministic sense after a number of days.

There are a variety of methods that can be employed in the solution of the equations. We shall put them into three broad categories—finite difference, spectral and finite-element techniques.

3.1 Finite differences

The first numerical techniques used in the solution of the primitive equations were based on finite differences. In this technique values and derivatives of the dependent variables are represented at discrete points on a grid. Usually the grid is regular in the coordinate system used, at least in the horizontal. In the vertical most centres have a non-uniform grid as it seems desirable to have finer resolution in the boundary layer and around the jet stream. Further enhancements to the performance (and to some extent the accuracy) of finite difference schemes can be made by staggering the dependent variables, i.e. by holding variables at different grid-points. Normally staggered schemes give a better simulation of geostrophic adjustment and they are either more accurate or more economical than equivalent non-staggered schemes.

In the design of any numerical scheme certain conditions need to be met to maintain stability. Since the primitive equations are nonlinear, they are prone to nonlinear computational instability under certain conditions. Nonlinear instability can be avoided by designing schemes in such a way as to conserve particular properties, normally enstrophy or kinetic energy. Such conservation properties are usually met by satisfying integral constraints that are also satisfied by the continuous system of equations. By maintaining these constraints in longer integrations, the statistical structure of the atmosphere is maintained and it may help to reduce systematic errors.

The design of conservative finite-difference schemes was pioneered by Arakawa (1966), Lilly (1964) and Sadourny (1975), and a review can be found in Arakawa (1984). Failure to conserve enstrophy, in particular, eventually leads to a spurious cascade of energy to smaller scales. It is possible to limit or control this false cascade by removing energy from these smaller scales by the use of lateral diffusion, but excessive lateral smoothing leads to enhanced energy dissipation.

To achieve conservation in the discretized system, successive terms need to cancel so that summing over a domain (equivalent to integrating the continuous equations) leaves only boundary values.

Conservation properties do not necessarily endow a particular scheme with increased local accuracy, which may be more advantageous for the forecasting of small-scale phenomena. Thus, the choice of a scheme with or without conservation is likely to be dictated by the problem being solved.

For global models, the most straightforward grid to use is based on lines of constant increments in latitude and longitude (Fig. 1). However, on such a grid the longitudinal points converge, and east–west resolution consequently increases as the poles are approached. Unless special measures are taken, this increase in resolution results in the violation of the CFL condition when explicit time-stepping schemes are used. In some formulations, the poles are singular points and usually have to be treated separately.

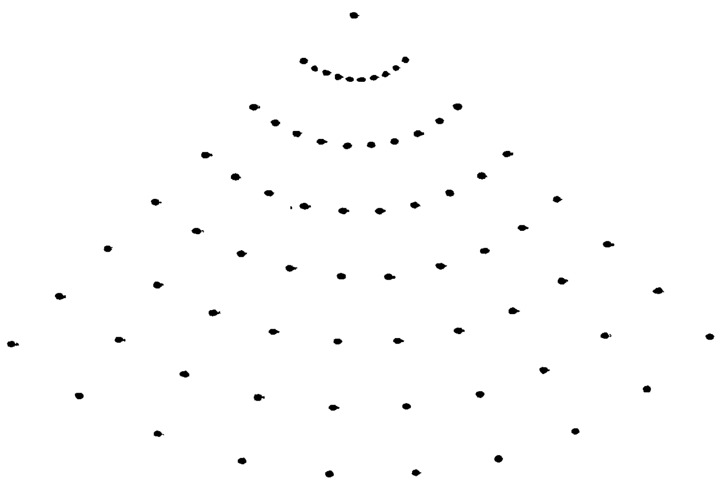

Figure 1Illustration of a regular latitude/longitude grid near a pole.

We can demonstrate the effects of converging meridians by considering a linearized version of the shallow-water equations

$$\frac{\partial u}{\partial t} + \frac{gS}{a\cos\varphi}\frac{\partial h}{\partial \lambda} = 0 \tag{38}$$

$$\frac{\partial v}{\partial t} + \frac{g}{a}\frac{\partial h}{\partial \varphi} = 0 \tag{39}$$

$$\frac{\partial h}{\partial t} + \frac{H}{a\cos\varphi}\left[S\frac{\partial u}{\partial \lambda} + \frac{\partial}{\partial \varphi}(v\cos\varphi)\right] = 0 \tag{40}$$

where we have inserted $S = S(\varphi)$ which will act to highlight the effects of longitudinal differencing and, if necessary, as a smoothing operator. We will examine the behaviour of two different schemes on an unstaggered grid, i.e. u, v and h are held at the same points. First, with a leapfrog scheme, the differentiation $\partial u/\partial t$ is replaced by $(u^{n+1} - u^{n-1})/2\Delta t$. We use central differences for the space differencing and, after substituting solutions of the form $u^n = \lambda^n \hat{u}\exp[\mathrm{i}(k\Delta\lambda + l\Delta\varphi)]$, etc we arrive at a system of equations, the determinant of which is

$$\begin{vmatrix} \lambda^2-1 & 0 & \lambda g S\dfrac{\Delta t}{(a\cos\varphi)\Delta\lambda}2i\sin(k\Delta\lambda) \\ 0 & \lambda^2-1 & \lambda f\dfrac{\Delta t}{a\Delta\varphi}2i\sin(l\Delta\varphi) \\ \lambda HS\dfrac{\Delta t}{(a\cos\varphi)\Delta\lambda}2i\sin(k\Delta\lambda) & \lambda H\dfrac{\Delta t}{a\Delta\varphi}2i\sin(l\Delta\varphi) & \lambda^2-1 \end{vmatrix} = 0 \quad (41)$$

(Note we have also used $\cos\varphi_{j+1} = \cos\varphi_{j-1} = \cos\varphi_j$ in the difference equation for h).

Evaluating the determinant, we obtain roots $\lambda = \pm 1$ and the solutions of

$$\lambda^4 - 2\lambda^2 + 1 + 4A\lambda^2 = 0 \quad (42)$$

$$\text{where } A = gH(\Delta t)^2\left[\frac{S^2\sin^2(k\Delta\lambda)}{a^2(\Delta\lambda)^2\cos^2\varphi} + \frac{\sin^2(l\Delta\varphi)}{a^2(\Delta\varphi)^2}\right] \quad (43)$$

$$\text{i.e. } \lambda^2 = 1 - 2A \pm \sqrt{(4A^2 - 4A)} \quad (44)$$

$$|\lambda| < 1 \ \text{ provided that A} < 1 \ \text{ or}$$

$$gH(\Delta t)^2\left[\frac{S^2\sin^2(k\Delta\lambda)}{a^2(\Delta\lambda)^2\cos^2\varphi} + \frac{\sin^2(l\Delta\varphi)}{a^2(\Delta\varphi)^2}\right] < 1 \ \text{ for all wave numbers } (k, l) \quad (45)$$

Reverting back to one dimension, this is simply $gH(\Delta t)^2/(\Delta x)^2 < 1$ or $\sqrt{(gH)}\Delta t/\Delta x < 1$, the usual CFL stability condition. For a regular Cartesian, two-dimensional grid we would have $\sqrt{(2gH)}\Delta t/\Delta x < 1$.

Now consider our latitude–longitude grid where as the poles are approached $a\Delta\lambda\cos\varphi$, becomes small and dominates the CFL condition. There are a number of ways to circumvent this problem. One of the simplest is to let the time step decrease towards the pole thereby maintaining the ratio $\Delta t/\Delta\lambda$, but this is prohibitively expensive. It is just as easy to restrict the number of waves in the solution, i.e. not letting the $\sin(k\Delta\lambda)$ term approach 1. Again, there are a variety of ways of doing this in practice. Essentially we obtain the Fourier components in the longitudinal direction and either truncate or smooth those modes (the higher wave numbers) that would be unstable by our stability criterion equation (45). We then perform an inverse transform to obtain our desired solution. Essentially we are trying to control the effect of $a\cos\varphi$ in the first tern of (45) $S^2\sin^2 k\Delta\lambda/[a^2(\Delta\lambda)^2\cos^2\varphi]$. For a particular latitude, we only retain those waves so that $\sin(k\Delta\lambda)/(a\Delta\lambda\cos^2\varphi) < 1/(a\Delta\lambda\cos\varphi_0)$, or $\sin(k\Delta\lambda) < \cos\varphi/\cos\varphi_0$, gives us the value of k that can be retained for a particular latitude. If we choose to truncate the solution at a particular wave number, the process is known as Fourier dropping. Alternatively, we can smooth the amplitude of a wave that would be unstable by using $S(k, \varphi)\sin((k\Delta\lambda) < \cos\varphi/\cos\varphi_0)$

We also have some freedom on how we apply the chopping or smoothing. We can apply the filter to the dependent variables, the tendencies or the increments. Arakawa and Lamb (1981) apply the smoothing operators S within the differencing as in equations (38) and (40).

It is instructive to repeat the above stability analysis using a forward–backward scheme for time differencing, i.e. the time differencing uses a forward scheme and the height term in the first two equations is at the latest time level. The same procedure as before gives.

$$\begin{vmatrix} \lambda - 1 & 0 & gS\dfrac{\Delta t}{(a\cos\varphi)\Delta\lambda}\mathrm{i}\sin(k\Delta\lambda) \\ 0 & 1 & f\dfrac{\Delta t}{a\Delta\varphi}\mathrm{i}\sin(l\Delta\varphi) \\ HS\dfrac{\Delta t}{(a\cos\varphi)\Delta\lambda}\mathrm{i}\sin(k\Delta\lambda) & \lambda H\dfrac{\Delta t}{a\Delta\varphi}\mathrm{i}\sin(l\Delta\varphi) & \lambda - 1 \end{vmatrix} = 0 \qquad (46)$$

Evaluating the determinant as before we find we require $A \le 4$ for $|\lambda| \le 1$ i.e. in one dimension $\sqrt{gH}\Delta t/\Delta x < 2$ and, for a regular Cartesian two-dimensional $\sqrt{2gH}\Delta t/\Delta x < 2$. The maximum time step for the forward–backward scheme is twice that for the leapfrog scheme and it has the further advantage of being a 2-level scheme.

As with the leapfrog scheme, the smoothing factor S plays the same role in determining those wave numbers we can retain by requiring $S(k, \varphi)\sin k\Delta\lambda < \cos\varphi/\cos\varphi_0$.

Another solution to the problem of converging meridians is to use a grid developed by Kurihara where points are skipped as the poles are approached, thereby roughly maintaining the same resolution. In its simplest form this leads to overlapping of grid boxes in the north–south direction, which complicates a little the differencing algorithms. A more serious drawback of such a grid appears to be associated with larger errors near the poles.

The above examples involved the use of unstaggered grids. However, the space differencing in equations (38) to (40) only involves variables at points adjacent to those required in the solution of the equations. Therefore, it is possible to carry the velocity components and height field at alternate points, thereby reducing the computation time and storage by half. The truncation error remains unaltered. By staggering the variables in this way we have effectively made $4\Delta x$ the shortest resolvable wavelength. If we want to include $2\Delta x$ waves then we can reduce the grid length by half and, in this case, for comparable computational effort as the unstaggered grid we increase the accuracy.

In two-dimensions, there are more options available when staggering the variables. One of the most recent reviews can be found in Janic and Mesinger (1984). The various choices of grids are denoted by the letters A to E. The A grid is the unstaggered arrangement. The other grids are as shown below.

B			C			D			E		
h		h	h	u	h	h	v	h	u, v	h	u, v
	u, v		v		v	u		u	h	u, v	h
h		h	h	u	h	h	v	h	u, v	h	u, v

The importance in the staggering of the variables is not just for computational efficiency, but is also related to the behaviour in the geostrophic adjustment process. By examining the dispersion properties for each of the grids, the relative merits of each of the grids can be assessed. Janic and Mesinger (1984) suggest that there is little to choose between the B and C grids whereas the unstaggered A grid is poor.

We have considered so far the adjustment or gravity-wave part of our system of equations. If necessary, the advective terms can be included in our simplified system. If we then carry out a stability analysis, the CFL criterion is usually modified by the addition of a velocity term such as $(U + \sqrt{gh})\Delta t/\Delta x$ compared with $\sqrt{gh}\Delta t/\Delta x$. Now typically $\sqrt{gh}$ has a value of about 300 m/s whereas maximum values of U are around 100 m/s. Hence, the stability condition is dominated by the gravity-wave speed. The addition of the nonlinear advection terms complicates the solution and makes it much more expensive to solve. However, since the stability condition for the winds is around a third as restrictive as the gravity-wave condition this expense could be reduced by somehow allowing the advection to set the time step rather than the gravity-wave speed. There are broadly two approaches. One is the semi-implicit approach, where the gravity-wave terms are treated implicitly and the advection terms are treated explicitly. Alternatively, a split–explicit approach can be adopted, where both parts are treated explicitly but separately so that differencing schemes suited to the relevant characteristics of each problem can be used. For example, a forward–backward scheme for the gravity-wave adjustment and a Lax–Wendroff or a Heun scheme for the advection step. If this approach is used, several adjustment steps can be taken for every advection step (typically 3 adjustment steps for each advection step).

3.2 Spectral technique

The operational ECMWF forecast model uses a spectral technique for its horizontal discretization. Over the past decade or so this technique has become the most widely used method of integrating the governing equations of numerical weather prediction over hemispheric or global domains. Following the development of efficient transform methods by Eliasen *et al*. (1970) and Orszag (1970), and the construction and testing of multi-level primitive-equation models (e.g. Bourke, 1974; Hoskins and Simmons, 1975; Daley *et al*., 1976), spectral models were introduced for operational forecasting in Australia and Canada during 1976. The technique has been utilized operationally in the USA since 1980, in France since 1982, and in Japan and at ECMWF since 1983. Implementation of a spectral model is planned in the Federal Republic of Germany. The method is also extensively used by groups involved in climate modelling.

A comprehensive account of the technique has been given by Machenhauer (1979), and a further description of the method has been given by Jarraud and Simmons (1984). Reference should be made to these or other reviews for further discussion of most of the points covered below.

In the usual application of the method, the basic prognostic variables are vorticity, divergence, temperature, a humidity variable, and the logarithm of surface pressure. Their horizontal representation is in terms of truncated series of spherical harmonic functions, whose variation is described by sines and cosines in the east–west and by associated Legendre functions in the north–south. The horizontal variation of a variable X is thus given by

$$X(\lambda, \mu) = \sum_{m=-M}^{M} \sum_{n=|m|}^{N} X_n^m \; P_n^m(\mu) \; \exp[im\lambda] \qquad (47)$$

where λ is the latitude and μ is the sine of the longitude. For the particular choice of normalization adopted at

$$P_n^m(\mu) = \sqrt{2n+1}\frac{(n-m)!}{(n+m)!}\frac{1}{2^n n!}(1-\mu^2)^{m/2}\frac{d^{n+m}}{d\mu^{n+m}}(\mu^2-1), \qquad m \ge 0$$

and

$$P_n^{-m}(\mu) = P_n^m(\mu) \; .$$

As X is a real variable, X_n^{-m} is equal to the complex conjugate of X_n^m, enabling the model to deal explicitly with the X_n^m for $m \ge 0$. The sum

$$\sum_{n=|m|}^{N} X_n^m \; P_n^m(\mu)$$

defines the "Fourier coefficients", $X^m(\mu)$ of the variable X.

It is becoming increasingly common for the so-called "triangular" truncation of the expansion to be used. This truncation is defined by $M = N = \text{constant}$, and gives uniform resolution over the sphere. The symbol “T*N*” is the usual way of defining the resolution of such a truncation; N being the smallest total wave number retained in the expansion. The smallest resolved half-wavelength in any particular direction is then $\pi a / N$ (320 km for T63, 190 km for T106), although the corresponding lateral variation is of larger scale.

Derivatives of a spectrally represented variable X are known analytically:

$$\frac{\partial X}{\partial \lambda} = \sum_{m=-M}^{M} \sum_{n=|m|}^{N} \mathrm{i} m X_n^m \, P_n^m(\mu) \, \exp[\mathrm{i} m \lambda] \tag{48}$$

and

$$\frac{\partial X}{\partial \mu} = \sum_{m=-M}^{M} \sum_{n=|m|}^{N} X_n^m \frac{\mathrm{d}P_n^m}{\mathrm{d}\mu} \exp[\mathrm{i} m \lambda] \tag{49}$$

where

$$(1-\mu^2)\frac{\mathrm{d}P_n^m}{\mathrm{d}\mu} = -n\varepsilon_{n+1}^m \, P_{n+1}^m + (n+1)\varepsilon_n^m \, P_{n-1}^m$$

with

$$\varepsilon_n^m = \left(\frac{n^2 - m^2}{4n^2 - 1}\right)^{\frac{1}{2}}$$

The orthogonality of the spherical harmonics enables the X_n^m to be determined from X according to the formula

$$X_n^m = \frac{1}{4\pi}\int_{-1}^{1}\int_{0}^{2\pi} X(\lambda, \mu) P_n^m(\mu) \, \exp[-\mathrm{i} m \lambda] \mathrm{d}\lambda \mathrm{d}\mu \tag{50}$$

The computational efficiency of the evaluation of the Fourier coefficients is enhanced for global models by writing the summation over n (known as the inverse Legendre transform) in the form

$$\sum_{n=|m|}^{N} X_n^m \, P_n^m(\mu) = \sum_{\substack{n=|m| \\ (n+m)\ \text{even}}}^{N} X_n^m \, P_n^m(\mu) + \sum_{\substack{n=|m|+1 \\ (n+m)\ \text{odd}}}^{N} X_n^m \, P_n^m(\mu) \tag{51}$$

Evaluating these two sums separately enables a simple evaluation of the inverse transform for the corresponding latitude in the opposite hemisphere:

$$\sum_{n=|m|}^{N} X_n^m \, P_n^m(-\mu) = \sum_{\substack{n=|m| \\ (n+m)\ \text{even}}}^{N} X_n^m \, P_n^m(\mu) - \sum_{\substack{n=|m|+1 \\ (n+m)\ \text{odd}}}^{N} X_n^m \, P_n^m(\mu) \tag{52}$$

Similarly, the latitudinal integral in (50), the direct Legendre transform, need be taken only over one hemisphere:

$$\begin{aligned}\int_{-1}^{1} X^m(\mu) P_n^m(\mu)\ \mathrm{d}\mu &= \int_0^1 [X^m(\mu) + X^m(-\mu)] P_n^m(\mu)\ \ \mathrm{d}\mu \quad \text{for } m+n \text{ even} \\ &= \int_0^1 [X^m(\mu) - X^m(-\mu)] P_n^m(\mu)\ \ \mathrm{d}\mu \quad \text{for } m+n \text{ odd}\end{aligned} \tag{53}$$

The spherical harmonics are eigenfunctions of the Laplacian operator on the sphere:

$$\nabla^2 \{P_n^m(\mu)\ \exp[\mathrm{i}m\lambda]\} = -\frac{n(n+1)}{a^2} P_n^m(\mu)\ \exp[\mathrm{i}m\lambda] \tag{54}$$

where a is the radius of the earth. This is utilized in deriving wind components from vorticity and divergence. If U and V are the eastward and northward velocity components multiplied by the cosine of latitude, the (relative) vorticity and divergence D are defined by

$$\xi = \frac{1}{a}\left\{\frac{1}{(1-\mu^2)}\frac{\partial V}{\partial \lambda} - \frac{\partial U}{\partial \mu}\right\} \tag{55}$$

and

$$D = \frac{1}{a}\left\{\frac{1}{(1-\mu^2)}\frac{\partial U}{\partial \lambda} + \frac{\partial V}{\partial \mu}\right\} \tag{56}$$

In terms of a stream function ψ and velocity potential χ :

$$U = \frac{1}{a}\left\{-(1-\mu^2)\frac{\partial \psi}{\partial \mu} + \frac{\partial \chi}{\partial \lambda}\right\}$$

$$V = \frac{1}{a}\left\{\frac{\partial \psi}{\partial \lambda} + (1-\mu^2)\frac{\partial \chi}{\partial \mu}\right\}$$

$$\xi = \nabla^2\psi \quad \text{and} \quad D = \nabla^2\chi$$

Thus

$$U = a \sum_{m=-M}^{M} \sum_{n=|m|}^{N} n^{-1}(n+1)^{-1}\left\{(1-\mu^2)\xi_n^m \frac{\mathrm{d}P_n^m}{\mathrm{d}\mu} - \mathrm{i}mD_n^m\ P_n^m\right\}\exp[im\lambda] \tag{57}$$

and

$$V = -a \sum_{m=-M}^{M} \sum_{n=|m|}^{N} n^{-1}(n+1)^{-1}\left\{\mathrm{i}m\xi_n^m\ P_n^m + (1-\mu^2)D_n^m \frac{\mathrm{d}P_n^m}{\mathrm{d}\mu}\right\}\exp[im\lambda] \tag{58}$$

The sequence of calculations for each time step of a spectral model can now be broadly summarized as follows. The analytical representation of basic fields (Eqs. (47)) is used to evaluate these fields, and derived fields such as horizontal velocities (Eqs. (48) and Eqs. (49)) and (in some implementations) temperature and moisture gradients, at an array of grid points. These grid-point values are used to compute contributions to the tendencies of the fields at the grid points from both resolved dynamical processes and from the parametrized processes. These tendencies are projected back to give tendencies of the spectral coefficients, enabling time-stepping to be completed. The transformation to and from grid-point values is particularly efficient in the east–west, for which Fast Fourier Transformation can be used. Gaussian quadrature is employed for the latitudinal integration used in the projection back to spectral space Eqs. (53); this requires that the grid in the north–south has a particular distribution (the so-called "Gaussian" latitudes) for each resolution, although this can be regarded as a regular grid for all practical applications of output grid-point products from spectral models at today's operational resolutions. An exact transformation of quadratic terms is achieved by using a grid which has a finer resolution than that of the spectral representation, with at least $(3N+1)$ points in the east–west and $(3N+1)/2$ from pole to pole for TN truncation (Fig. 2). If, as is generally (but not necessarily) the case, the physical parametrizations are computed on this grid, then prognostic fields such as surface temperature or snow cover, and output fields such as precipitation, are defined and updated on this grid.

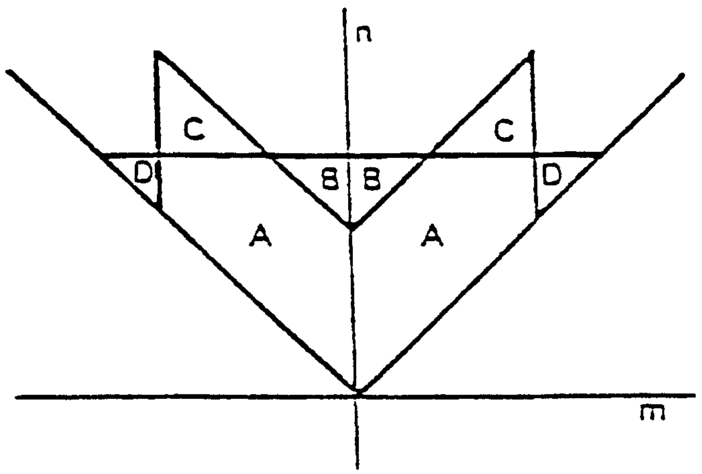

Figure 2. Illustration of various spectral truncations: Triangular truncation $\mathrm{T}M = A + B + D$ and Rhomboidal truncation $\mathrm{R}M = A + C$

In the formulation adopted at ECMWF, complete tendencies of the temperature, moisture and logarithm of surface pressure are computed in grid-point space, and transformed directly into the corresponding tendencies of spectral coefficients. For vorticity and divergence, integration by parts is used. The wind tendencies can be written in the form

$$\frac{\partial U}{\partial t} = F_u - \frac{1}{a}\frac{\partial G}{\partial \lambda} \tag{59}$$

and

$$\frac{\partial V}{\partial t} = F_v - \frac{(1-\mu^2)}{a}\frac{\partial G}{\partial \mu} \tag{60}$$

where F_u, F_v and G are quantities that can readily be computed in grid-point space.

Using equations (50), (55) and (56), (59) and (60) yield

$$\begin{aligned}\frac{\partial \xi_n^m}{\partial t} &= \frac{1}{4\pi a}\int_{-1}^{1}\int_{0}^{2\pi}\left\{\frac{1}{1-\mu^2}\frac{\partial F_v}{\partial \lambda}-\frac{\partial F_u}{\partial \mu}\right\}P_n^m(\mu)\,\exp[-\mathrm{i}m\lambda]\mathrm{d}\lambda\mathrm{d}\mu \\ &= \frac{1}{4\pi a}\int_{-1}^{1}\int_{0}^{2\pi}\frac{1}{1-\mu^2}\left\{\mathrm{i}mF_vP_n{}^m(\mu)+(1-\mu^2)F_u\frac{\mathrm{d}P_n^m}{\mathrm{d}\mu}\right\}\exp[-\mathrm{i}m\lambda]\mathrm{d}\lambda\mathrm{d}\mu\end{aligned} \tag{61}$$

and

$$\begin{aligned}\frac{\partial D_n^m}{\partial t} &= \frac{1}{4\pi a}\int_{-1}^{1}\int_{0}^{2\pi}\left\{\frac{1}{1-\mu^2}\frac{\partial F_u}{\partial \lambda}+\frac{\partial F_v}{\partial \mu}-a\nabla^2G\right\}P_n^m(\mu)\,\exp[-\mathrm{i}m\lambda]\mathrm{d}\lambda\mathrm{d}\mu \\ &= \frac{1}{4\pi a}\int_{-1}^{1}\int_{0}^{2\pi}\frac{1}{1-\mu^2}\left\{\mathrm{i}mF_uP_n^m(\mu)-(1-\mu^2)F_v\frac{\mathrm{d}P_n^m}{\mathrm{d}\mu}\right\}\exp[-\mathrm{i}m\lambda]\mathrm{d}\lambda\mathrm{d}\mu \\ &\quad+\frac{n(n+1)}{4\pi a^2}\int_{-1}^{1}\int_{0}^{2\pi}GP_n^m(\mu)\,\exp[-\mathrm{i}m\lambda]\mathrm{d}\lambda\mathrm{d}\mu\end{aligned} \tag{62}$$

The fact that the spherical harmonics are eigenfunctions of the Laplacian operator makes it relatively simple to implement an efficient semi-implicit treatment of gravity-wave terms. It is also straightforward to implement linear forms of "horizontal" diffusion along the coordinate surfaces defined by the vertical discretization. Such diffusion is widely used in spectral models, with largely satisfactory results. There can, however, as in finite-difference models, be problems associated with diffusion along coordinate surfaces which slope significantly in the vicinity of steep terrain, and the introduction of other forms of diffusion may require significant effort and computational cost.

Recent developments of the spectral technique have been along a number of lines. Apart from computational refinements of the type discussed in the following section, the technique has lent itself to some further gains in time-stepping efficiency in high-resolution applications (Simmons *et al.*, 1988), and there is promise of further increases of efficiency with the use of a semi-Lagrangian treatment of advection (Ritchie, 1988). The applicability of the technique has been widened by the development of limited-area spectral models (e.g. Tatsumi, 1986), and of a stretched coordinate within the framework of a global model (Courtier and Geleyn, 1988, following Schmidt, 1977).

3.3 Finite-element techniques

Finite-elements are much less widespread in operational NWP when compared with either spectral or grid-point models. RPN in Canada have the most practical experience in using finite-elements for both horizontal and vertical discretization. A review article by Staniforth (1987) gives an introduction and contains useful references.

There is an experimental version of the Centre's model that uses finite elements in the vertical and, apart from noise problems at the upper boundary, this version appears to give greater accuracy more cheaply than increasing vertical resolution using finite differences.

4. VERTICAL COORDINATES

So far, height above mean sea level has been used as the vertical coordinate in our system of equations. For mid-latitude synoptic-scale disturbances the Coriolis force and pressure-gradient force are in approximate balance—the geostrophic relationship which is $f\mathbf{k}\times\mathbf{V} = -(1/\rho)\nabla p$, a diagnostic relationship relating the velocity field to the pressure gradient.

However, the density varies with latitude and height which make the above equation less easy to use than an alternative system which uses pressure as the vertical coordinate. Other coordinates are more useful for numerical techniques in solving the complete equations of motion. We can derived a system of equations for a generalized vertical coordinate which is assumed to be related to the height z by a single-valued monotonic function. This was derived by Kasahara (1974).

$$\zeta = \zeta(x, y, z, t) \quad \text{or} \quad z = z(x, y, \zeta, t)$$

We have

$$\left(\frac{\partial A}{\partial s}\right)_\zeta = \left(\frac{\partial A}{\partial s}\right)_z + \frac{\partial A}{\partial z}\left(\frac{\partial z}{\partial s}\right)_\zeta \quad \text{where } s = x, y, \text{or } t \tag{63}$$

and

$$\frac{\partial A}{\partial z} = \frac{\partial A}{\partial \zeta}\frac{\partial \zeta}{\partial z} \tag{64}$$

Thus

$$\left(\frac{\partial A}{\partial s}\right)_\zeta = \left(\frac{\partial A}{\partial s}\right)_z + \frac{\partial A}{\partial \zeta}\frac{\partial \zeta}{\partial z}\left(\frac{\partial z}{\partial s}\right)_\zeta \tag{65}$$

Using the above, we have

$$\left(\frac{\partial A}{\partial t}\right)_\zeta = \left(\frac{\partial A}{\partial t}\right)_z + \frac{\partial A}{\partial \zeta}\frac{\partial \zeta}{\partial z}\left(\frac{\partial z}{\partial t}\right)_\zeta \tag{66}$$

$$\nabla_\zeta A = \nabla_z A + \frac{\partial A}{\partial \zeta}\frac{\partial \zeta}{\partial z}\nabla_\zeta z \tag{67}$$

$$\nabla_\zeta \cdot \mathbf{V} = \nabla_z \cdot \mathbf{V} + \frac{\partial \mathbf{V}}{\partial \zeta}\frac{\partial \zeta}{\partial z} \cdot \nabla_\zeta z \tag{68}$$

The total derivative $\mathrm{d}/\mathrm{d}t$ can be transformed into the ζ system using (66) and (67), thus

$$\frac{\mathrm{d}}{\mathrm{d}t} = \left(\frac{\mathrm{d}}{\mathrm{d}t}\right)_\zeta + \mathbf{V}\cdot\nabla_\zeta + \left[w - \left(\frac{\partial z}{\partial t}\right)_\zeta - \mathbf{V}\cdot\nabla_\zeta\right]\frac{\partial \zeta}{\partial z}\frac{\partial}{\partial \zeta} \tag{69}$$

However, by definition, the total derivative in the ζ system is

$$\frac{\mathrm{d}}{\mathrm{d}t} = \left(\frac{\partial}{\partial t}\right)_\zeta + \mathbf{V}\cdot\nabla_\zeta + \dot{\zeta}\frac{\partial}{\partial\zeta} \tag{70}$$

where $\dot{\zeta} = \mathrm{d}\zeta/\mathrm{d}t$ is the vertical velocity in the ζ system.

From (69) and (70) we have

$$\dot{\zeta} = \frac{\partial\zeta}{\partial z}\left[w - \left(\frac{\partial z}{\partial t}\right)_\zeta - (\mathbf{V}\cdot\nabla_\zeta z)\right] \tag{71}$$

Using (67). We can write the horizontal pressure forces as

$$-\frac{1}{\rho}\nabla_z p = -\frac{1}{\rho}\nabla_\zeta p + \frac{1}{\rho}\frac{\partial p}{\partial z}\nabla_\zeta z = -\frac{1}{\rho}\nabla_\zeta p - \nabla_\zeta\Phi \tag{72}$$

where $\Phi = gz$ is the geopotential. The hydrostatic equation becomes

$$\frac{\partial p}{\partial\zeta} = -\rho\frac{\partial\Phi}{\partial\zeta} \tag{73}$$

The horizontal equation of motion (neglecting friction) becomes

$$\frac{\mathrm{d}V}{\mathrm{d}t} = -\frac{1}{\rho}\nabla_\zeta p - \nabla_\zeta\Phi - f\mathbf{k}\times\mathbf{V} \tag{74}$$

To derive the continuity equation, from (71) we have

$$w = \left(\frac{\partial z}{\partial t}\right)_\zeta + V\cdot\nabla_\zeta z + \dot{\zeta}\frac{\partial z}{\partial\zeta} \tag{75}$$

Thus

$$\begin{aligned}\frac{\partial w}{\partial z} &= \frac{\partial w}{\partial\zeta}\frac{\partial\zeta}{\partial z} = \frac{\partial\zeta}{\partial z}\left[\frac{\partial}{\partial\zeta}\left(\frac{\partial z}{\partial t}\right)_\zeta + \frac{\partial\mathbf{V}}{\partial\zeta}\cdot\nabla_\zeta z + \mathbf{V}\cdot\nabla\frac{\partial z}{\partial\zeta} + \dot{\zeta}\frac{\partial}{\partial\zeta}\left(\frac{\partial z}{\partial\zeta}\right) + \frac{\partial z}{\partial\zeta}\frac{\partial\dot{\zeta}}{\partial\zeta}\right]\\ &= \frac{\partial\zeta}{\partial z}\left[\frac{\mathrm{d}}{\mathrm{d}t}\left(\frac{\partial z}{\partial\zeta}\right) + \frac{\partial\mathbf{V}}{\partial\zeta}\cdot\nabla_\zeta z\right] + \frac{\partial\dot{\zeta}}{\partial\zeta}\end{aligned} \tag{76}$$

Using (66) and (67) and substituting in the continuity equation

$$\frac{\mathrm{d}}{\mathrm{d}t}(\ln\rho) + \nabla\cdot V + \frac{\partial w}{\partial z} = 0$$

we have

$$\frac{\mathrm{d}}{\mathrm{d}t}(\ln\rho) + \nabla_\zeta\cdot\mathbf{V} - \frac{\partial\mathbf{V}}{\partial\zeta}\frac{\partial\zeta}{\partial z}\cdot\nabla_\zeta z + \frac{\partial\zeta}{\partial z}\left[\frac{\mathrm{d}}{\mathrm{d}t}\left(\frac{\partial z}{\partial\zeta}\right) + \frac{\partial\mathbf{V}}{\partial\zeta}\cdot\nabla_\zeta z\right] + \frac{\partial\dot{\zeta}}{\partial\zeta}$$

i.e.

$$\frac{\mathrm{d}}{\mathrm{d}t}\ln\left(\rho\frac{\partial z}{\partial\zeta}\right)+\nabla_\zeta\cdot\mathbf{V}+\frac{\partial\dot{\zeta}}{\partial\zeta} = 0 \qquad (77)$$

or

$$\frac{\mathrm{d}}{\mathrm{d}t}\ln\left(\frac{\partial p}{\partial\zeta}\right)+\nabla_\zeta\cdot\mathbf{V}+\frac{\partial\dot{\zeta}}{\partial\zeta} = 0 \qquad (78)$$

Alternatively, by expanding (77) and using the hydrostatic equation, we can obtain

$$\frac{\partial}{\partial\zeta}\left(\frac{\partial p}{\partial t}\right)+\nabla_\zeta\cdot\left(\mathbf{V}\frac{\partial p}{\partial\zeta}\right)+\frac{\partial}{\partial\zeta}\left(\dot{\zeta}\frac{\partial p}{\partial\zeta}\right) = 0 \qquad (79)$$

The above equations for a generalized vertical coordinate may now be used to examine alternative coordinate systems.

4.1 Pressure coordinate $\zeta = p$

$\nabla_\zeta p = \nabla_p p = 0$ and $\partial p/\partial p = 1$ so that the equation of motion (74) becomes

$$\frac{\mathrm{d}V}{\mathrm{d}t} = -\nabla_p\Phi-f\mathbf{k}\times\mathbf{V} \qquad (80)$$

and the hydrostatic equation is

$$\frac{\partial\Phi}{\partial p} = -\frac{1}{\rho} \qquad (81)$$

The first term in the continuity equation (77) vanishes, so that

$$\nabla_p\cdot V+\frac{\partial\omega}{\partial p} = 0 \qquad (82)$$

where $\omega = \mathrm{d}p/\mathrm{d}t = \dot{p}$ is the vertical velocity. Integrating (80) from $p = 0$ where $\omega = 0$, to an arbitrary level, p, yields

$$\omega = \int_0^p\nabla_p\cdot\mathbf{V}\mathrm{d}p \qquad (83)$$

At the surface we assume no normal flux so that

$$\omega_\mathrm{s} = \frac{\mathrm{d}p_\mathrm{s}}{\mathrm{d}t} = \frac{\partial p_\mathrm{s}}{\partial t}+\mathbf{V}_\mathrm{s}\cdot\nabla p_\mathrm{s} = -\int_0^{p_s}(\nabla_p\cdot\mathbf{V}\mathrm{d}p) \qquad (84)$$

In the pressure system, the geostrophic approximation gives

$$f\mathbf{k}\times\mathbf{V} = -\nabla_p\Phi \qquad (85)$$

This relates the horizontal velocity to the geopotential gradient and, since there is no longer a dependence on density, the same gradient implies the same wind at any height.

4.2 Sigma coordinates

The lower boundary condition (82) is not easy to apply in practice. To circumvent this problem, Phillips suggested the use of $\sigma = p/p_*$ as the vertical coordinate. The hydrostatic equation becomes

$$p_* = -\rho\frac{\partial\Phi}{\partial\sigma} \tag{86}$$

and the equation of motion becomes

$$\frac{\partial\mathbf{V}}{\partial t} + \mathbf{V}\cdot\nabla\mathbf{V} + \dot{\sigma}\frac{\partial\mathbf{V}}{\partial\sigma} = -\nabla_\sigma\Phi - \frac{RT}{p_*}\nabla p_* - f\mathbf{k}\times\mathbf{V} \tag{87}$$

The continuity becomes

$$\frac{\mathrm{d}(\ln p_*)}{\mathrm{d}t} + \nabla_\sigma\cdot\mathbf{V} + \frac{\partial\dot{\sigma}}{\partial\sigma} = 0$$

Expanding the first term and rearranging we have

$$\frac{\partial p_*}{\partial t} = -\nabla\cdot(p_*V) = \frac{\partial(p\dot{\sigma})}{\partial\sigma} \tag{88}$$

The boundary conditions are $\dot{\sigma} = 0$ at $\sigma = 0$ and 1, so that integrating (86) from $\sigma = 0$ to 1 gives

$$\frac{\partial p_*}{\partial t} = -\int_0^1 \nabla\cdot(p_*V)\mathrm{d}\sigma \tag{89}$$

i.e. the surface pressure tendency is given by the mass divergence integrated over the entire atmosphere. Integrating (86) from $\sigma = 0$ to an arbitrary level gives our equation for $\dot{\sigma}$, viz

$$-p_*\dot{\sigma} = \sigma\frac{\partial p_*}{\partial t} + \int_0^\sigma \nabla\cdot(p_*V)\mathrm{d}\sigma \tag{90}$$

Although the lower boundary condition in the sigma coordinate system is easier to apply than in pressure coordinates, the system does have a drawback in the terms for the horizontal pressure force. In pressure coordinates the pressure force is simply the gradient of geopotential whereas in sigma coordinates it is the difference of two terms which are large in magnitude when compared with the result, i.e.

$$-\nabla\Phi - \frac{RT}{p_*}\nabla p_* \tag{91}$$

In designing a difference scheme for the above, care must be taken in selecting a scheme that minimizes the error in the difference between the terms. Even so, where the gradient in orography is steep, it is almost impossible to devise a consistent scheme that is free from appreciable error.

Over steep orography, the sigma levels slope appreciably even in the stratosphere (see Fig. 3) and the problems with the horizontal pressure force remain. It seems, therefore, that a scheme which combines the advantage of sigma coordinates near the surface and pressure coordinate in the stratosphere may prove advantageous. Such schemes exist and are known as hybrid coordinates.

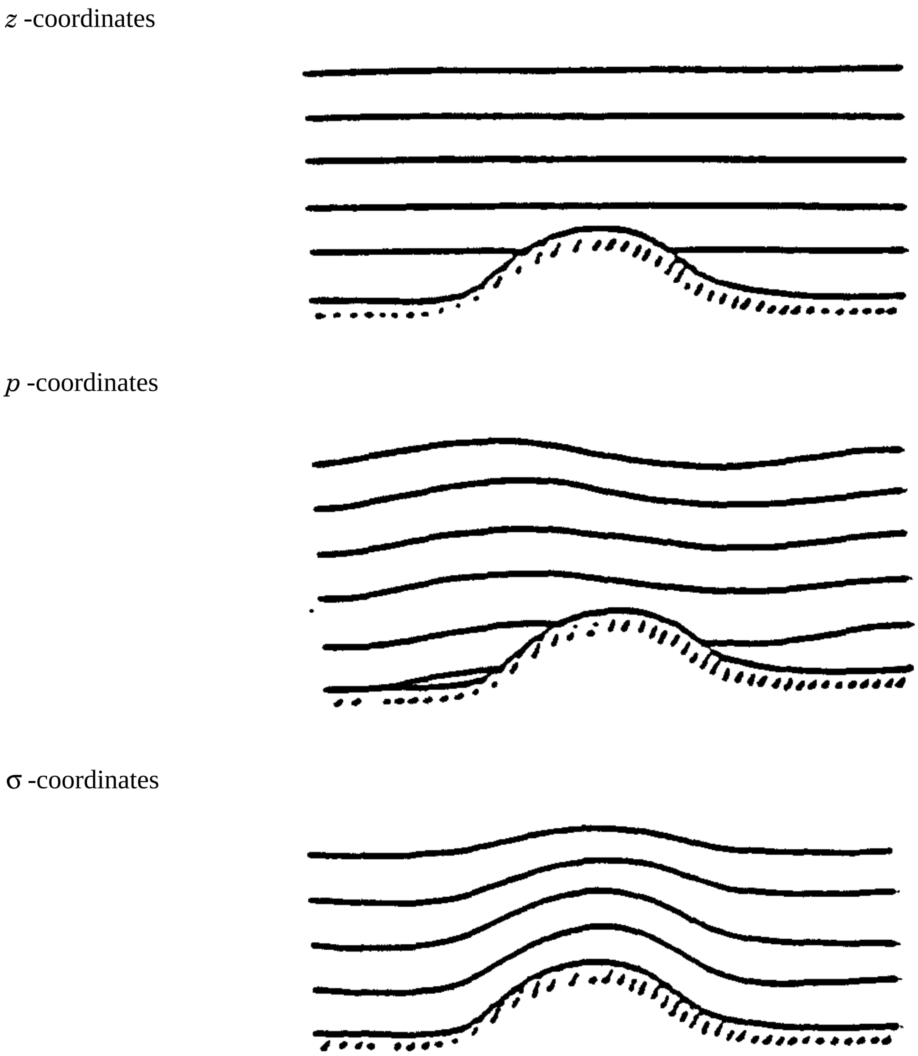

Figure 3Illustration of the three vertical coordinate systems.

4.3 Hybrid coordinates

There are various ways of defining a coordinate system that has the properties of sigma coordinates in the lower atmosphere and pressure in the stratosphere. Arakawa and Lamb (1977) use the definition

$$\eta_k = \frac{(p_k - p_{\mathrm{I}})}{\pi} \tag{92}$$

where

$$\pi = \begin{cases} p_{\mathrm{I}} - p_{\mathrm{T}} & \text{for} \quad p_{\mathrm{T}} \le p \le p_{\mathrm{I}} \\ p_* - p_{\mathrm{I}} & \text{for} \quad p_{\mathrm{I}} \le p \le p_* \end{cases} \tag{93}$$

where p_{I} is an interfacial pressure (e.g. near the tropopause) and p_{T} is the pressure at the top of the model. In fact, setting $p_{\mathrm{I}} = p_{\mathrm{T}} = 0$ gives the standard σ-system. In this hybrid system the boundary conditions are applied at $\eta = \pm 1$.

Simmons and Burridge (1981) showed that an alternative way of defining hybrid coordinates was to define the half-levels by the relation

$$p_{k+1/2} = A_{k+1/2} p_0 + B_{k+1/2} p_* \tag{94}$$

where p_0 is a constant pressure. This form of coordinate allows a direct control over the flattening of the coordinate surfaces as the pressure decreases. Note that we can define sigma coordinates or hybrid coordinates as in (89) in the same manner as (91), so that for sigma coordinates

$$p_{k+1/2} = \sigma_{k+1/2} p_* \tag{95}$$

An alternative form of hybrid coordinates equivalent to the Arakawa–Lamb system is

$$\begin{aligned} p_{k+1/2} &= p_{\mathrm{I}+1/2} \frac{\eta_{k+1/2}}{\eta_{\mathrm{I}+1/2}} \quad \text{for} \quad \eta_{k+1/2} \le \eta_{\mathrm{I}+1/2} \\ p_{k+1/2} &= p_{\mathrm{I}+1/2} + \frac{(\eta_{k+1/2} - \eta_{\mathrm{I}+1/2})(p_* - p_{\mathrm{I}+1/2})}{(1 - \eta_{\mathrm{I}+1/2})} \end{aligned} \tag{96}$$

The reason for defining the half-levels $p_{k+1/2}$ in this way is due to the appearance of terms involving $\partial p / \partial \eta$ in the equations which, when discretized, become $\Delta p_k = p_{k+1/2} - p_{k-1/2}$ (see, for example, the continuity equation (78)).

4.4 Isentropic coordinates

In Θ coordinates (isentropic), for dry adiabatic motions, potential temperature Θ is conserved, so that the energy equation becomes $\mathrm{d}\Theta / \mathrm{d}t = 0$ and the isentropic surfaces become material surfaces.

From (74), the horizontal pressure force is $-(1/\rho)\nabla_\Theta p - \nabla_\Theta \Phi$

Using $\Theta T / \Pi$ where $\Pi = (p/p_0)^\kappa$, we have

$$\nabla_\Theta(\ln\Theta) = 0 = \nabla_\Theta(\ln T) - \kappa \nabla_\Theta(\ln p)$$

i.e.

$$-\frac{1}{p}\nabla_\Theta p = \frac{C_p}{RT}\nabla_\Theta T$$

Hence, using equation of state, we have

$$-\frac{1}{\rho}\nabla_\Theta p = \nabla_\Theta C_p T \tag{97}$$

The horizontal pressure force can thus be written as $-\nabla_\Theta(C_pT+\Phi)$ or $-\nabla_\Theta M$ where $M = C_pT+\Phi$ is called the Montgomery stream function. The hydrostatic equation (73) can be written $\partial p/\partial\Theta = -\rho(\partial\Phi/\partial\Theta)$.

Again, using the definition for Θ above we have

$$\ln\Theta = \ln T - \kappa\ln\frac{p}{p_0}$$

Differentiating w.r.t. Θ gives

$$\frac{1}{\Theta} = \frac{1}{T}\frac{\partial T}{\partial\Theta} - \frac{R}{C_p p}\frac{\partial p}{\partial\Theta}$$

Substituting for $\partial p/\partial\Theta$ in the hydrostatic equation, using the equation of state and rearranging, we obtain

$$\frac{\partial}{\partial\Theta}(C_pT+\Phi) = \frac{C_pT}{\Theta} \tag{98}$$

or alternatively

$$\frac{\partial M}{\partial\Theta} = \Pi$$

For the continuity equation it is convenient to use one of the forms (78) or (79) with Θ replacing ζ

The boundary conditions are, at the top $\dot{\Theta} = 0$ and at the earth's surface $\dot{\Theta} = \partial\Theta/\partial t + \mathbf{V}_* \cdot \nabla\Theta_*$.

The isentropic coordinate shows (as with the pressure coordinate) the advantage of a simpler pressure gradient force, but also the disadvantage at the surface which is intersected by Θ-surfaces. It is possible to introduce yet another hybrid scheme using σ-coordinates near the surface and Θ-coordinates away from the surface. However, how to join or overlap these systems is not as straightforward as in the sigma–pressure type of hybrid coordinate. For further details see Bleck (1978) and references therein.

5. VERTICAL DISCRETIZATION

Even though computer power has increased enormously in the last 10 to 15 years the vertical resolution in primitive equation models is quite low, 10 to 20 levels in the vertical being typical and these levels are generally irregularly spaced to take account of the strong variation of atmospheric quantities in the vertical. For example, high resolution near the earth's surface is required with many formulations to represent the transition between the turbulence region close to the surface and the free atmosphere.

However, there are a number of problems arising from the choice of vertical coordinate system and the distribution of discrete model levels in the vertical. Firstly, the inevitable presence of an artificial upper boundary can eventually contaminate forecasts. The conclusion of several theoretical studies is that having the model top at zero pressure is, in some respects, as a result of inevitable finite-difference errors, equivalent to having the model top at some small finite non-zero pressure. On the other hand, it has been pointed out that the influence of lowering the upper boundary is not damaging to the structure of the planetary waves in the troposphere, if it is placed no lower than the middle stratosphere and if the model has several layers in the stratosphere where damping effects can attenuate waves reflected from the top.

Experimentally (Mechoso *et al*., 1984), it has been shown that the impact of the upper boundary on forecasts is considerable at the uppermost model levels in all cases, and that lowering the upper boundary to the lower stratosphere can affect significantly middle and lower tropospheric forecasts in some cases. The comparison between integrations with 16 and 19-level models described below supports these results.

The detrimental effects of using terrain-following coordinates have been the subject of study for many years. Small-scale errors and computational noise where the coordinate surfaces are steep or rapidly changing in the horizontal are generated as a result of the discrete approximations made for the terms in the partial differential equations. The particular problem of the pressure gradient force is well known. The horizontal pressure gradient force (see equation (91)) in a σ-coordinate model is given by

$$-\nabla\Phi - \frac{RT}{p_*}\nabla p_*$$

and near steep orography the near cancellation of the two terms in this expression is a potential source of large spatial truncation errors.

These errors can be decreased to some extent by formulating carefully the differencing approximations for the hydrostatic equation and pressure gradient force, but cannot be totally eliminated as long as a terrain-following coordinate is used. There is also some concern about the accurate representation of the advection of quantities such as moisture near significant irregularities in the coordinate surface, and there are also problems in the treatment of horizontal diffusion terms. Overall, the undesirable effects can be partly removed by using a hybrid coordinate system which changes smoothly from a terrain-following specification near the lower boundary, to a horizontal or isobaric definition in the upper troposphere and stratosphere. An alternative method has also been developed, using quasi-horizonal coordinates and representing mountains as steps, although this has not been tested exhaustively in practice as yet. A full discussion of the numerical problems associated with terrain following coordinate systems is given in Mesinger and Janic (1984) and Simmons and Burridge (1981).

In comparison with the scheme used for horizontal discretization, the vertical discretization scheme in use in the majority of large-scale models of the atmosphere can be described as rudimentary based, as they generally are, on simple finite differences that provide second-order accuracy, at best, with the irregularity of the level spacing reducing the local accuracy to first order.

Very few attempts have been made to employ the use of analytical functions that are continuously differentiable and defined globally; the two really potentially useful approaches—by Francis (1972) using Laguerre polynomials and by Machenhauer and Daley (1972) who used Legendre functions—have not led to practical schemes for numerical models of the atmosphere. The use of Laguerre polynomials leads to severe stability criteria, whereas the use of Legendre polynomials gives rise to computational problems at the upper boundary.

In contrast to the global functional approaches of Francis and Machenhaur and Daley, the use of local functional approaches based on Galerkin implementations of finite elements has been fairly successful. A successful finite element formulation for the vertical discretization in σ-coordinate primitive equation models was described by Staniforth and Daley (1977), and a 36-hour forecast from real data was presented to demonstrate the viability of the method.

The remainder of this section is devoted to a description of a vertical finite differencing scheme for a σ-coordinate model.

5.1 Vertical differencing schemes for baroclinic primitive equation models

In this subsection I shall discuss the methodology underlying the design of many vertical differencing schemes.

The approach is based on the imposition of some important conservation laws.

The equations introduced in Section 1 may be rewritten as

$$\frac{\partial p_s}{\partial t} + \nabla_\sigma \cdot (p_s \mathbf{v}) + \frac{\partial}{\partial \sigma}(p_s \dot{\sigma}) = 0 \quad \text{continuity of mass} \tag{99}$$

$$\frac{\partial \mathbf{v}}{\partial t} + Z\mathbf{k} \times \mathbf{v} + \dot{\sigma}\frac{\partial \mathbf{v}}{\partial \sigma} + \nabla_\sigma(\Phi + E) + RT\nabla_\sigma(\ln p_s) = 0 \quad \text{momentum} \tag{100}$$

$$\frac{\partial}{\partial t}(p_s C_p T) + \nabla_\sigma \cdot (p_s \mathbf{v} C_p T) + \frac{\partial}{\partial \sigma}(p_s \sigma \dot{C}_p T) - \frac{RT\omega}{\sigma} = 0 \quad \text{thermodynamics} \tag{101}$$

$$\frac{\partial \Phi}{\partial(\ln \sigma)} = -RT \quad \text{hydrostatic equation} \tag{102}$$

with

$$\begin{aligned} Z &= f + \frac{1}{a\cos\varphi}\left\{\frac{\partial v}{\partial \lambda} - \frac{\partial}{\partial \varphi}(u\cos\varphi)\right\} \\ E &= \frac{1}{2}(u^2 + v^2) = \frac{1}{2}(\mathbf{v}\cdot\mathbf{v}) \\ \omega &= p_s\dot{\sigma} + \sigma\left(\frac{\partial p_s}{\partial t} + \mathbf{v}\cdot\nabla_\sigma p_s\right) \end{aligned} \tag{103}$$

For completeness we again state the upper and lower "no flux" boundary conditions

$$\begin{aligned} (p_s\dot{\sigma})_{\sigma=0} &= 0 \\ (p_s\dot{\sigma})_{\sigma=1} &= 0 \end{aligned} \tag{104}$$

For our discussion we shall require mass and energy conservation. In particular, we want the work done by pressure forces to be balanced by the changes in the total potential energy arising from $(RT\omega)/\sigma$ (the ω-term).

The integrated continuity equation is

$$\frac{\partial p_s}{\partial t} = -\nabla_\sigma \cdot \int_0^1 p_s \mathbf{v}\, d\sigma \tag{105}$$

The divergence term in (105) integrates to zero over the globe, which means that the total mass is conserved.

A "kinetic energy" equation can be derived from the momentum equations in the form

$$\begin{gathered} p_s\mathbf{v}\cdot\frac{\partial \mathbf{v}}{\partial t} + p_s\dot{\sigma}\mathbf{v}\cdot\frac{\partial \mathbf{v}}{\partial \sigma} + p_s\mathbf{v}\nabla_\sigma E + p_s\mathbf{v}\cdot(\nabla_\sigma\Phi + RT\nabla_\sigma \ln p_s) = 0 \\ \text{or} \\ p_s\frac{\partial E}{\partial t} + p_s\dot{\sigma}\frac{\partial E}{\partial \sigma} + p_s\mathbf{v}\nabla_\sigma E + p_s\mathbf{v}\cdot(\nabla_\sigma\Phi + RT\nabla_\sigma \ln p_s) = 0 \end{gathered} \tag{106}$$

Using the continuity equation, (99) and (106) may be rewritten as

$$\frac{\partial}{\partial t}(p_s E) + \boxed{\nabla_\sigma \cdot (p_s \mathbf{v} E) + \frac{\partial}{\partial \sigma}(p_s \dot{\sigma} E)} + p_s \mathbf{v} \cdot (\nabla_\sigma \Phi + RT \nabla_\sigma \ln p_s) = 0 \qquad (107)$$

In order to construct the total energy equation we need to express the pressure gradient terms in an alternative form. Using the continuity and hydrostatic equations we have

$$\begin{aligned} p_s \mathbf{v} \cdot \nabla_\sigma \Phi &= \nabla_\sigma \cdot (p_s \mathbf{v} \Phi) + \Phi(\nabla_\sigma \cdot p_s \mathbf{v}) \\ &= \nabla_\sigma \cdot (p_s \mathbf{v} \Phi) + \Phi \left\{ \frac{\partial p_s}{\partial t} + \frac{\partial}{\partial \sigma}(p_s \dot{\sigma}) \right\} \\ &= \nabla_\sigma \cdot (p_s \mathbf{v} \Phi) + \frac{\partial}{\partial \sigma}\left\{ \Phi\left(\sigma \frac{\partial p_s}{\partial t} + p_s \dot{\sigma} \right) \right\} - \frac{\partial \Phi}{\partial \sigma}\left(\sigma \frac{\partial p_s}{\partial t} + p_s \dot{\sigma} \right) \end{aligned} \qquad (108)$$

Combining (107) and (108) we have

$$\begin{aligned} \frac{\partial (p_s E)}{\partial t} + \boxed{\nabla_\sigma \cdot (p_s \mathbf{v} E) + \frac{\partial}{\partial \sigma}(p_s \dot{\sigma} E) + \nabla_\sigma \cdot (p_s \mathbf{v} \Phi) + \frac{\partial}{\partial \sigma}\left\{ \Phi\left(\sigma \frac{\partial p_s}{\partial t} + p_s \dot{\sigma} \right) \right\}} \\ - \frac{\partial \Phi}{\partial t}\left(\sigma \frac{\partial p_s}{\partial t} + p_s \dot{\sigma} \right) + RT p_s \mathbf{v} \cdot \nabla_\sigma \ln p_s = 0 \end{aligned}$$

Now

$$\begin{aligned} & -\frac{\partial \Phi}{\partial t}\left(\sigma \frac{\partial p_s}{\partial t} + p_s \dot{\sigma} \right) + RT p_s \mathbf{v} \cdot \nabla_\sigma \ln p_s \\ &= \frac{RT}{\sigma}\left(\sigma \frac{\partial p_s}{\partial t} + p_s \dot{\sigma} \right) + RT \mathbf{v} \cdot \nabla_\sigma p_s = \frac{RT\omega}{\sigma} \end{aligned}$$

Addition of the kinetic energy equation and the flux form of the thermodynamic equation (equation (101)) and integration from $\sigma = 0$ to 1 gives

$$\frac{\partial}{\partial t}\left\{ p_s \Phi_s + \int_0^1 p_s (E + C_p T) \mathrm{d}\sigma \right\} + \nabla_\sigma \cdot \int_0^1 p_s \mathbf{v}(E + C_p T + \Phi) \mathrm{d}\sigma = 0 \qquad (109)$$

Equation (109) is an expression of the energy conservation law for the σ -system (99) to (103). The horizontal divergence tern in (109) integrates to zero over the whole globe, which means that the total energy, potential plus kinetic, is conserved.

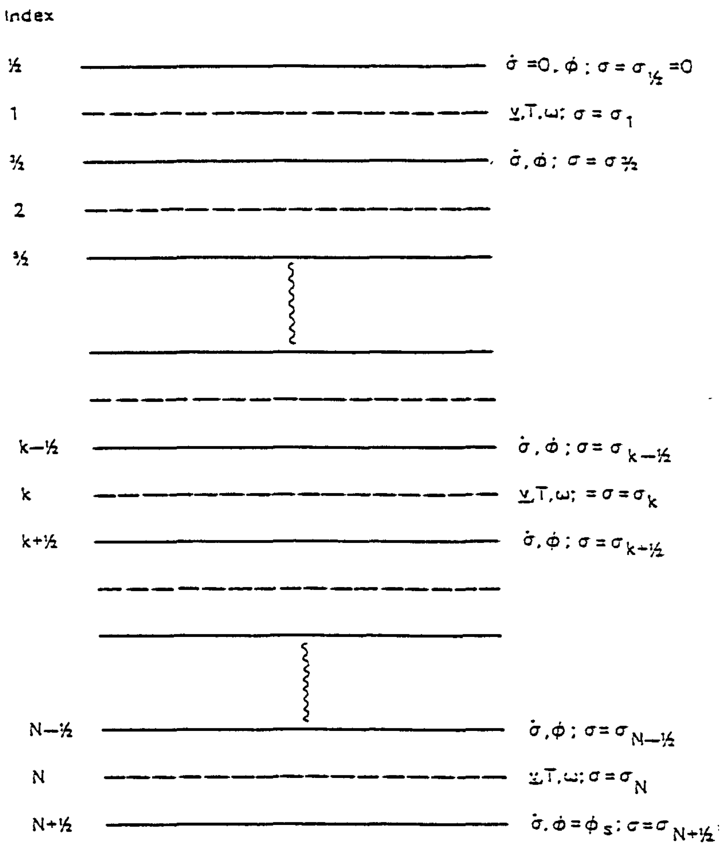

Figure 4Vertical disposition of variables

The disposition of variables and the grid structure in the vertical for the σ-coordinate model we shall be using is illustrated in Figs. 4 and 5 . The primary variables, $\mathbf{v}$ and T, are kept at the full levels and the vertical velocity $\dot{\sigma}$ and the geopotential are kept at half levels. The variable grid spacing $\Delta\sigma_k$ is defined by

$$\Delta\sigma_k = \sigma_{k+1/2} - \sigma_{k-1/2} \tag{110}$$

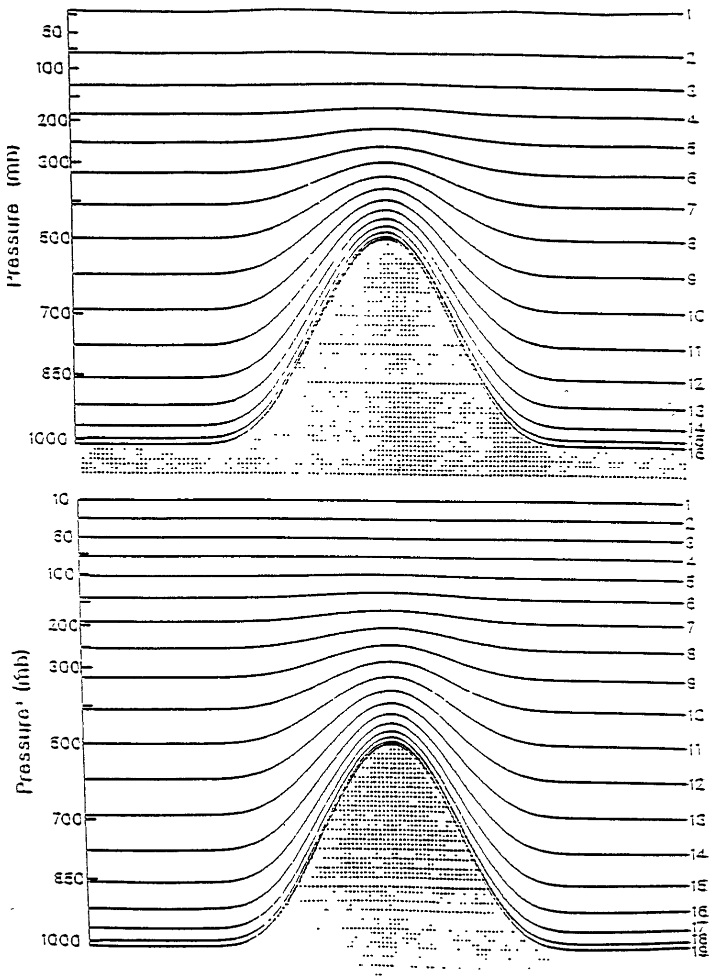

Figure 5Vertical distribution of levels for the 16-level (top) and 19-level (bottom) models.

(i) **The equation of continuity**. The continuity equation is taken in the form

$$\frac{\partial p_s}{\partial t} + \nabla_\sigma \cdot (p_s \mathbf{v}_k) + \frac{\Delta(p_s \dot{\sigma})_k}{\Delta\sigma_k} = 0 \qquad (111)$$

Multiplying (111) by $\Delta\sigma_k$ and summing (integration) from $k = 1, \ldots, K$ gives

$$\sigma_{k+1/2}\frac{\partial p_s}{\partial t} + \sum_{k=1}^{K} [\nabla_\sigma \cdot (p_s \mathbf{v}_k)\Delta\sigma_k + p_s \dot{\sigma}_{k+1/2}] = 0 \qquad (112)$$
$$(p_s \dot{\sigma}_{1/2} = 0)$$

For $K = N$ we have

$$\frac{\partial p_s}{\partial t} = -\sum_{k=1}^{K} \nabla_\sigma \cdot (p_s \mathbf{v}_k)\Delta\sigma_k = -\nabla_\sigma \cdot \sum_{n=1}^{N} (p_s \mathbf{v}_k)\Delta\sigma_k \qquad (113)$$

Equation (113) is a finite difference analogue of (105), which obviously conserves the total (global) mass of the model atmosphere.

(ii) **Energy conservation**. The finite difference momentum equation is

$$\frac{\partial \mathbf{v}_k}{\partial t} + Z\mathbf{k} \times \mathbf{v} + \frac{1}{2}\left\{\frac{\dot{\sigma}_{k+1/2}(\mathbf{v}_{k+1} - \mathbf{v}_k) + \dot{\sigma}_{k-1/2}(\mathbf{v}_k - \mathbf{v}_{k-1})}{\nabla_\sigma \sigma_k}\right\} + \nabla_\sigma\{\Phi_k + E_k\} + RT_k \nabla_\sigma \ln p_s = 0 \qquad (114)$$

where $\Phi_k = \alpha_k \Phi_{k+1/2} + \beta_k \Phi_{k-1/2}$ with $\alpha_k + \beta_k = 1$.

The finite difference kinetic energy equation is

$$p_s \mathbf{v}_k \cdot \frac{\partial \mathbf{v}_k}{\partial t} + \frac{1}{2} p_s \mathbf{v}_k \cdot \left\{\frac{\dot{\sigma}_{k+1/2}(\mathbf{v}_{k+1} - \mathbf{v}_k) + \dot{\sigma}_{k-1/2}(\mathbf{v}_k - \mathbf{v}_{k-1})}{\Delta \sigma_k}\right\} + p_s \mathbf{v}_k \cdot \nabla_\sigma E_k + p_s \mathbf{v}_k \cdot \{\nabla_\sigma \Phi_k + RT \nabla_\sigma \ln p_s\} = 0$$

and this may be rewritten as

$$p_s \frac{\partial E_k}{\partial t} + \frac{1}{2}\left\{\frac{p_s \dot{\sigma}_{k+1/2} \mathbf{v}_{k+1} \cdot \mathbf{v}_k - p_s \dot{\sigma}_{k-1/2} \mathbf{v}_k \cdot \mathbf{v}_{k-1}}{\Delta \sigma_k}\right\} - \frac{1}{2} \mathbf{v}_k \cdot \mathbf{v}_k \frac{\Delta (p_s \dot{\sigma})_k}{\Delta \sigma_k} + p_s \mathbf{v}_k \cdot \nabla_\sigma E_k + p_s \mathbf{v}_k \cdot \{\nabla_\sigma \Phi_k + RT \nabla_\sigma \ln p_s\} = 0 \qquad (115)$$

Using the finite difference continuity equation we may rewrite equation (115) in the flux form

$$\frac{\partial}{\partial t}(p_s E_k) + \nabla_\sigma \cdot (p_s \mathbf{v}_k E_k) + \Delta_\sigma \left(\frac{p_s \dot{\sigma} \widehat{\mathbf{v}^2}^{\sigma}}{2}\right)_k + p_s \mathbf{v}_k \cdot \{\nabla_\sigma \Phi_k + RT \nabla_\sigma \ln p_s\} = 0 \qquad (116)$$

where $\left(\widehat{\mathbf{v}^2}^{\sigma}\right)_{k+1/2} = \mathbf{v}_{k+1} \cdot \mathbf{v}_k$ (geometric mean) .

In order to derive the analogue of the identity (108) we need a hydrostatic equation; we use

$$\left(\frac{\Delta_\sigma \Phi}{\Delta \ln \sigma}\right)_k = -RT \qquad (117)$$

For the finite difference model we have

$$\begin{aligned}
p_s\mathbf{v}_k\cdot\nabla_\sigma\Phi_k &= \nabla_\sigma\cdot(p_s\mathbf{v}_k\Phi_k)-\Phi_k\nabla_\sigma\cdot(p_s\mathbf{v}_k)\\
&= \nabla_\sigma\cdot(p_s\mathbf{v}_k\Phi_k)+\Phi_k\left\{\frac{\partial p_s}{\partial t}+\frac{\Delta_\sigma(p_s\dot{\sigma})_k}{\Delta\sigma_k}\right\}\\
&= \nabla_\sigma\cdot(p_s\mathbf{v}_k\Phi_k)+\frac{\Phi_k}{\Delta\sigma_k}\Delta_\sigma\left(\sigma\frac{\partial p_s}{\partial t}+p_s\dot{\sigma}\right)_k\\
&= \nabla_\sigma\cdot(p_s\mathbf{v}_k\Phi_k)+\frac{\Delta_\sigma\left\{\Phi\left(\sigma\frac{\partial p_s}{\partial t}+p_s\dot{\sigma}\right)\right\}_k}{\Delta\sigma_k}\\
&\quad -\frac{(\Delta_\sigma\Phi)_k}{\Delta\sigma_k}\left[\beta_k\left(\sigma\frac{\partial p_s}{\partial t}+p_s\dot{\sigma}\right)_{k+1/2}+\alpha_k\left(\sigma\frac{\partial p_s}{\partial t}+p_s\dot{\sigma}\right)_{k-1/2}\right]
\end{aligned}\tag{118}$$

Note:

$$\begin{aligned}
\Phi_k(A_{k+1/2}-A_{k-1/2}) &= (\alpha_k\Phi_{k+1/2}+\beta_k\Phi_{k-1/2})(A_{k+1/2}-A_{k-1/2})\\
&= (\Phi_{k+1/2}A_{k+1/2}-\Phi_{k-1/2}A_{k-1/2})-(\Phi_{k+1/2}-\Phi_{k-1/2})(\beta_kA_{k+1/2}+\alpha_kA_{k-1/2})
\end{aligned}$$

If we require total energy conservation then the form of the last term in (118) is a constraint on our choice for the ω term, $\kappa T\omega/\sigma$, in the thermodynamic equation.

The thermodynamic equation for our model is

$$p_s\frac{\partial T_k}{\partial t}+p_s\mathbf{v}_k\cdot\nabla_\sigma T_k+p_s\frac{1}{2}\left\{\frac{\dot{\sigma}_{k+1/2}(T_{k+1}-T_k)+\dot{\sigma}_{k-1/2}(T_k-T_{k-1})}{\Delta\sigma_k}\right\}-\left(\frac{\kappa T\omega}{\sigma}\right)_k = 0 \tag{119}$$

If the ω term is chosen to maintain energy conservation we have

$$\begin{aligned}
\left(\frac{\kappa T\omega}{\sigma}\right)_k &= \frac{1}{C_p}\left(\frac{RT\omega}{\sigma}\right)_k\\
&= \frac{1}{C_p}\left[-\frac{(\Delta\Phi)_k}{\Delta\sigma_k}\left\{\beta_k\left(\sigma\frac{\partial p_s}{\partial t}+p_s\dot{\sigma}\right)_{k+1/2}+\alpha_k\left(\sigma\frac{\partial p_s}{\partial t}+p_s\dot{\sigma}\right)_{k-1/2}\right\}+RT_k\mathbf{v}_k\cdot\nabla p_s\right]\\
&= \frac{1}{C_p}\left[RT_k\left(\frac{\Delta\ln\sigma}{\Delta\sigma}\right)_k\left\{\beta_k\left(\sigma\frac{\partial p_s}{\partial t}+p_s\dot{\sigma}\right)_{k+1/2}+\alpha_k\left(\sigma\frac{\partial p_s}{\partial t}+p_s\dot{\sigma}\right)_{k-1/2}\right\}+RT_kp_s\mathbf{v}_k\cdot\nabla\ln p_s\right]
\end{aligned}\tag{120}$$

The term $(\Delta\ln\sigma/\Delta\sigma)_k$ can be interpreted as a definition of $1/\sigma_k$ for the model.

From (120) we note that we still have a degree of freedom remaining, namely the choice of α_k and β_k, subject to $\alpha_k+\beta_k = 1$. These weights can be chosen in such a way that no spurious angular momentum is generated by pressure forces, Simmons and Burridge (1981).

REFERENCES

Books and collections.

Dutton, J.A., 1986: *The ceaseless wind: An introduction to the theory of the atmospheric motion*. Paperback edition.

ECMWF Seminar 1983: *Numerical methods for weather prediction*. Vol. 1 and Vol. 2.

Holton, J.R., 1979: *An introduction to dynamic meteorology.* Second edition.

Chang, J., (Editor), 1977: *General circulation models of the atmosphere*. Methods in Computational Physics 17.

Haltiner, G.J. and R.T. Williams, 1980: *Numerical prediction and dynamic meteorology.* Second Edition.

Journal papers.

Arakawa, A., 1966: Computational design for long-term numerical integration of the equations of fluid motion: two-dimensional incompressible flow. Part 1. *J. Comp. Phys*. 1, p119.

Arakawa, A. and V.R. Lamb, 1977: Computational design and the basic dynamical processes of the UCLA general circulation Model. Methods in Computational Physics 17. p173.

Arakawa, A. and V.R. Lamb, 1981: A potential enstrophy and energy conserving scheme for the shallow water equations. *Mon. Wea. Rev.*, 109. p18.

Arakawa, A., 1984a: The use of integral constraints in designing finite-difference schemes for the two-dimensional advection equation. ECMWF Seminar 1983 Numerical Methods for Weather Prediction. Vol. 1. p159.

Arakawa, A., 1984b: Vertical differencing of filtered models. ECMWF Seminar 1983 Numerical Methods for Weather Prediction. Vol. 1. p183.

Arakawa, A., 1984c: Vertical differencing of the primitive equations. ECMWF Seminar 1983 Numerical Methods for Weather Prediction. Vol. 1. p207.

Bell, R.S. and A. Dickinson, 1987: The Meteorological Office operational numerical weather prediction system. Meteorological Office Sci. Pap. 41 London HMSO.

Bleck, R., 1978: On the use of hybrid vertical coordinates in numerical weather prediction models. *Mon. Wea. Rev.*, 106. p1233.

Bourke, W., 1974: A multi-level spectral model 1: Formulation and hemispheric integrations. *Mon. Wea. Rev.*, 102. p687.

Bourke, W., B. McAvaney, K. Puri and R. Thurling, 1977: Global Modelling of Atmospheric Flow by Spectral Methods. Methods in Computational Physics 17. p267.

Corby, G.A., A. Gilchrist and P.R. Rowntree, 1977: United Kingdom Meteorological Office five-level general circulation model. Methods in Computational Physics 17. p67.

Courtier, P. and J-F. Geleyn, 1988: A global numerical weather prediction model with variable resolution: Application to the shallow-water equations. *Quart. J. Roy. Met. Soc*., 114. p1321.

Daley, R., C. Girard, J. Henderson and 1. Simmonds, 1976: Short term forecasting with a multi-level spectral primitive equation model. Atmosphere 14. p98.

Davies, H.C., 1976: A lateral boundary formulation for multi-level prediction models. *Quart. J. Roy. Met. Soc.*, 102. p405.

Davies, H.C., 1984: Techniques for limited area modelling. ECMWF Seminar 1983 Numerical Methods for Weather Prediction. Vol. 2. p213.

Dey, C.H., 1978: Noise suppression in a primitive equation prediction model. *Mon. Wea. Rev.*, 106. p159.

Eliasen, E., B. Machenhauer and E. Ramussen, 1970: On a numerical method for the integration of the hydrodynamical equations with a spectral representation of the horizontal fields. Rep. No. 2 Institut for Teoretisk Meteorologi, Univ. of Copenhagen.

Francis, P.E., 1972: The possible use of Laguerre polynomials for representing the vertical structure of numerical models of the atmosphere. *Quart. J. Roy. Met. Soc*., 98. p662.

Francis, P.E., 1975: The use of a multipoint filter as a dissipative mechanism in a numerical model of the general circulation of the atmosphere. *Quart. J. Roy. Met. Soc*., 101. p567.

Gadd, A.L, 1978a: A split-explicit integration scheme for numerical weather prediction. *Quart. J. Roy. Met. Soc*., 104, p569.

Gadd, A.J., 1978b: A numerical advection scheme with small phase speed errors. *Quart. J. Roy. Met. Soc.*, 104. p583.

Gadd, A.J., 1980: Two refinements of the split explicit integration scheme. *Quart. J. Roy. Met. Soc.*, 106. p215.

Hoskins, B.J. and A.J. Simmons, 1975: A multi-layer spectral model and the semi-implicit method. *Quart. J. Roy. Met. Soc.*, 101. p637.

Janic, Z. and F. Mesinger, 1984: Finite-difference methods for the shallow water equations on various horizontal grids. ECMWF Seminar 1983 Numerical Methods for Weather Prediction. Vol. 1. p29.

Jarraud, M. and A.J. Simmons, 1984: The spectral technique. ECMWF Seminar 1983 Numerical Methods for Weather Prediction. Vol. 2. pl. K911berg, P.W. and J.K. Gibson. 1977: Multi-level limited-area forecasts using boundary zone relaxation. WGNE Progress Rep. No. 15, p48.

Kasahara, A., 1974: Various vertical coordinate systems used for Numerical Weather Prediction. *Mon.Wea.Rev.*, 102, p509.

Kasahara, A., 1977: Computational aspects of numerical models for weather prediction and climate simulation. Methods in Computational Physics 17. pl.

Kirkwood, E. and J. Demme, 1977: Some effects of the upper boundary condition and vertical resolution on modelling forced stationary planetary waves. *Mon. Wea. Rev.*, 105. p133.

Kurihara, Y., 1965: Numerical integration of the primitive equations on a spherical grid. *Mon. Wea. Rev.*, 93, p399.

Lilly, D.K., 1964: Numerical solutions for the shape-preserving two-dimensional thermal convection element. *J. Atmos. Sci.*, 21. p83.

Machenhauer, B., 1979: The spectral method. In: Numerical Methods used in Atmospheric Models. GARP Publlication Series No. 17, Vol. II.

Machenhauer, B. and R. Daley, 1972: A bamclinic primitive equation model with spectral representation in three-dimensions. Rep. No. 4. Institut for Teoretisk Meteorologi, Univ. of Copenhagen.

Mechoso, C.R., M.J. Suarez, K. Yamazaki, A. Kitoh and A. Arakawa, 1984: Effects of the stratosphere on tropospheric forecasts. In: Report of the seminar on progress in numerical modelling and the understanding of predictability as a result of the global weather experiment. WMO GARP Special Report No. 43.

Mesinger, F. and A. Arakawa, 1976: Numerical methods used in atmospheric models. GARP Publication Series No. 17, Vol. I.

Mesinger, F. 1981: Horizontal advection schemes of a staggered grid- an enstrophy and energy conserving model. Mon.Wea.Rev., 109. p467.

Mesinger, F. and Z. Janic, 1984: Finite-difference schemes for the pressure-gradient force and for the hydrostatic equation. ECMWF Seminar 1983 Numerical methods for weather prediction. Vol. I. p103.

Orszag, S.A., 1970: Transform method for the calculation of vector coupled sums: application to the spectral form of the vorticity equation. *J. Atmos. Sci*. 27. p890.

Phillips, N.A., 1957: A coordinate system having some special advantages for numerical forecasting. *J. Meteor.* 14. p184.

Phillips, N.A., 1959: Numerical integration of the primitive equations on the hemisphere. *Mon. Wea. Rev.*, 87. p333.

Phillips, N.A., 1973: Principles of large-scale numerical weather prediction. Article in: Dynamic Meteorology: Editor P. Morel: p3.

Ritchie, H., 1988: Application of the semi-Lagrangian method to a spectral model of the shallow-water equations. *Mon. Wea. Rev.*,116. p1587.

Sadourny, R., 1975: The dynamics of finite-difference models of the shallow-water equations. *J. Atmos. Sci*. 32. p680.

Schmidt, F., 1977: Variable fine mesh spectral global models. *Beit. Phys. Atmos*. 50. p211.

Simmons, A.J. and D.M. Burridge, 1981: An energy and angular-momentum conserving vertical finite-difference scheme and hybrid vertical coordinates. *Mon. Wea. Rev.*, 109. p758.

Simmons, A.J. and R Snuffing, 1981: An energy and angular-momentum conserving vertical finite-difference scheme, hybrid coordinates and medium-range weather prediction. ECMWF Tech. Rep. No. 28.

Simmons, A.J. and D. Dent, 1989: The ECMWF multi-tasking weather prediction model. To appear in Computer Physics Reports.

Simmons, A.J., D.M. Burridge, M. Jarraud, C. Girard and W. Wergen, 1988: The ECMWF medium-range prediction models. Development of the numerical formulations and the impact of increased resolution. *Meteorol. Atmos. Phys.* 40. p28.

Staniforth, A. and R.W. Daley, 1977: A finite-element formulation for the vertical discretization of sigma coordinate primitive equation models. *Mon. Wea. Rev.*, 105. p1108.

Staniforth, A. and H.L. Mitchell, 1977: A semi-implicit finite-element barotropic model. *Mon.Wea.Rev.*, 105. p154.

Staniforth, A., 1987: Review: Formulating efficient finite-element codes for flows in regular domains. *Int. J. Num. Meth. Fluids* 7. p l.

Washington, W.M. and D.L. Williamson, 1977: A description of the NCAR Global Circulation Models. *Methods in Computational Physics* 17. pl 11.

Williamson, D.L. 1976: Linear stability of finite-difference approximations on a uniform latitude-longitude grid with Fourier filtering. *Mon. Wea. Rev.*, 104. p31.

